

FLUID RADIATION EFFECTS IN THE TRANSIENT HOT-WIRE TECHNIQUE

Measurement of thermal conductivity of propane

Y. Shi¹, L. Sun¹, F. Tian¹, J. E. S. Venart^{1,2} and R. C. Prasad^{1*}

¹University of New Brunswick, Saint John, NB, E2L 4L5, Canada

²University of New Brunswick, Fredericton, NB, E3B 5A3, Canada

The transient hot-wire technique is widely used for absolute measurements of the thermal conductivity of fluids. Refinement of this method has resulted in a capability for accurate and simultaneous measurement of both thermal conductivity and thermal diffusivity together with a determination of the specific heat. However, these measurements, especially those for the thermal diffusivity, may be significantly influenced by fluid radiation.

The present work investigates the effect of fluid radiation on the measurements of the thermal conductivity of propane. Recently developed corrections have been used to examine this assumption and rectify the influence of even weak fluid radiation. Measurements at 372 K with a hot-wire instrument demonstrate the presence of radiation effects in both the liquid and vapor phase. The influence is much more pronounced in liquid propane at 15.5 MPa than in the vapor phase at 881.5 kPa. The technique employed to obtain radiation-free thermal conductivity measurements is described.

Keywords: argon, natural convection, *n*-pentane, propane, thermal conductivity, thermal diffusivity, thermal radiation, transient hot wire technique

Introduction

Thermophysical properties such as thermal conductivity, thermal diffusivity, specific heat and other thermal parameters of materials obtained by various measurement and/or thermal analysis techniques are important for industrial applications as well as for materials characterization. Therefore, many authors [1–7] have investigated the thermal properties including thermal conductivity, thermal diffusivity and thermal stability together with spectral and microscopic studies to characterize materials. The thermal conductivity of fluids, in particular, has direct use in the design of heat exchangers. It is essential, therefore, to develop instruments as well as techniques for its accurate experimental measurement. The transient hot-wire instrument provides rapid and accurate measurements of the fluid thermal conductivity [8–10]. A series of corrections [9] must be applied to account for the differences between the actual and ideal heat transfer models. This includes thermal radiation effects which depend on the surrounding fluid if it is transparent to or absorbs thermal radiation. Earlier transient line-source measurements have considered propane to be transparent to thermal radiation. In this work, it will be shown that the influence of fluid radiation is similar to that in toluene and *n*-pentane which have been shown to

strongly absorb thermal radiation [9, 10]. Radiation-corrected measurements for propane show significant deviations from NIST [11] which does not include these corrections.

Methodology

The transient hot-wire instrument consists of a very thin and long wire vertically submerged in the test fluid. A constant current through the wire results in a transient temperature rise of the wire due to heat dissipation into the surrounding fluid. The ideal temperature rise of the fluid ΔT at $r=a$, the wire-fluid interface at time t is obtained from the transient solution of Fourier's law for an infinite line source [8] and is approximated by

$$\Delta T = \frac{q}{4\pi\lambda(\rho, T)} \ln \frac{4\alpha t}{a^2 C} \quad (1)$$

where

$$\Delta T = \Delta T_w + \sum \delta T_i$$

and $\sum \delta T_i$ are appropriate corrections to the measured temperature rise, ΔT_w , q is the power per unit length applied to the wire, λ is the thermal conductivity, $\alpha = \lambda / (\rho C_p)$ is the thermal diffusivity, ρ is the density, and C_p is the isobaric heat capacity (all for the test

* Author for correspondence: prasad@unb.ca

fluid), T is the temperature, t is the measured elapsed time, a is the radius of hot-wires, with $C=1.781 \dots$ the exponential of Euler's constant. One of the corrections accounts for the thermal radiation δT_{rad} .

For fluids which are transparent to thermal radiation, the radiation effect can be corrected by [12]

$$\delta T_{\text{rad}} = \frac{8\pi a \varepsilon_p \sigma T_0^3 \Delta T^2}{q} \quad (2)$$

However, for fluids which absorb radiation, it has been shown that the dominant correction term in the heat flux gradient arises from the emission of radiation from the heated fluid [12]. With this limitation, the solution for the temperature rise of the hot wire, $\Delta T(a, t)$, for finite radius a at time t can be given as [9]:

$$\Delta T(a, t) = \frac{q}{4\pi\lambda_2} \ln \frac{4\alpha_2 t}{a^2 C} - \frac{q}{4\pi\lambda_2} f \alpha_2 t - \frac{q a^2}{8\pi\lambda_2 \alpha_2 t} + \frac{q f a^2}{16\pi\lambda_2} \left(\frac{-\pi^2}{6} + \ln^2 \frac{4\alpha_2 t}{a^2 C} \right) \quad (3a)$$

where

$$f = \frac{B}{\alpha_2} \text{ and } B = \frac{16Kn^2\sigma T_0^3}{(\rho C_p)_2} \quad (3b)$$

K is the mean absorption coefficient, n is the refractive index of the test fluid, and σ is the Stephan–Boltzmann constant. K and n are assumed independent of temperature.

The correction for fluid radiation, therefore, is [9]:

$$\delta T_{\text{rad}} = \frac{q}{4\pi\lambda_2} f \alpha_2 t + \frac{q a^2}{8\pi\lambda_2 \alpha_2 t} - \frac{q f a^2}{16\pi\lambda_2} \left(\frac{-\pi^2}{6} + \ln^2 \frac{4\alpha_2 t}{a^2 C} \right) \quad (4)$$

Use of suitable B-values in Eqs (3b) and (4) allows the temperature rise of the wire to be corrected for thermal radiation and provide for the determination of radiation-free thermal properties of the test medium.

Experimental

A transient hot-wire cell designed for measurements of both thermal conductivity and thermal diffusivity [9, 10] was used. The cell uses two wires, each of different length, for end effect compensation (Fig. 1). Hot-wire specifications are listed in Table 1. The apparatus [9, 10] includes a pressurizing system and an isothermal block to maintain the test fluid at a desired pressure (up to 70 MPa) and temperature (120–500 K).

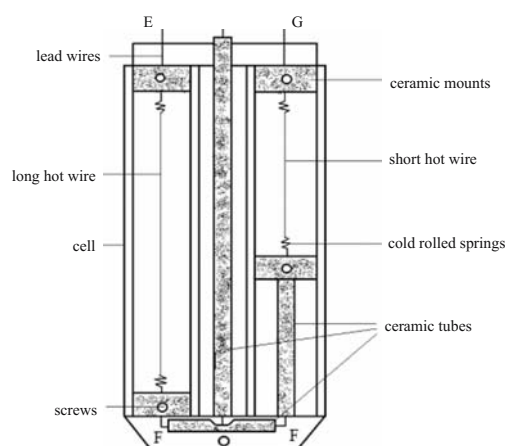


Fig 1 Schematic diagram of the hot-wire cell

Table 1 Hot-wire specifications [10]

Calibration equation: $R=R_0(1+a_1T+a_2T^2+b_1P+b_2P^2)$; $T/^\circ\text{C}$, P/kPa		
Wire specifications and calibration coefficient		
Wire parameter	Long wire (R_l)	Short wire (R_s)
Material	Platinum	Platinum
Purity/%	99.999	99.999
Length/m	0.08549±0.00001	0.023997±0.00001
Radius/ μm	6.35±1.1%	6.35±1.1%
R_0/Ω	0.00396989	0.0039487
a_1	62.22233	24.73335
a_2	$-5.272545 \cdot 10^{-7}$	$-6.00775 \cdot 10^{-7}$
b_1	$-6.098034 \cdot 10^{-8}$	$-5.691791 \cdot 10^{-8}$
b_2	$7.634 \cdot 10^{-13}$	$7.116 \cdot 10^{-13}$

The electrical system shown in Fig. 2 [9] includes a data acquisition/control unit (HP3497A), a dc power supply (HP6625A), an integrating voltmeter (HP3458A), an external trigger unit (HP3437A), and a C-MOS digital switch between the 'dummy' and the 'measurement' circuit. In Fig. 2, the long wire, R_l , is represented by the element connected across EF and the short wire, R_s , by the element across terminals GF . Terminals E , F and G of the platinum wires are also shown in Fig. 1 with terminal F common to both the long and the short wires.

HP3497A provides a low current (1, 0.1 and 0.01 mA) source for balancing the bridge, an integrating voltmeter with integration times of 0.167, 1.67, and 16.67 ms, and digital switches. HP6625A provides a high-stability fast response power supply with up to 75 watts of power, with voltage up to 50 volts and currents up to 2 Amps. The apparatus and measurement techniques are described in reference [9, 10]. HP3458A multimeter is used for accurate measurement of DC voltage, DC current and resis-

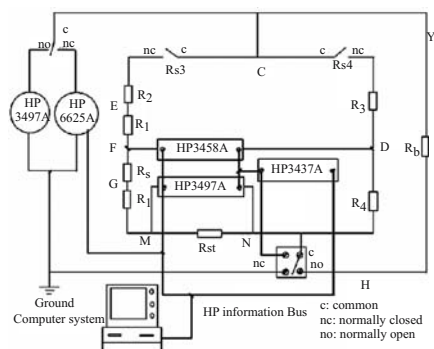


Fig. 2 Electrical system and the measurement bridge

tance as well as the transient imbalance of the bridge introduced by the step-current through the hot-wire resulting in change in their temperature and resistance. HP3437A is a system voltmeter, capable of delaying an external trigger from 0 to 1 sec and of generating up to 9999 triggers at rates of 1 Hz through 5700 Hz per second [9]. It is used to trigger HP3497A, HP3458A, and C-MOS switch to initiate step current through the hot wires and begin simultaneous measurements of both the current and the voltage across the bridge elements.

Results and discussion

Measurements with nitrogen

Thermal conductivity, thermal diffusivity and specific heat of nitrogen were determined with this system and the results compared with NIST [11] and Sun [13]. The maximum and average deviations are shown in Table 2 and the deviation plot is shown in Fig. 3 [10, 14]. These results demonstrate the reliability of the measurement system.

Thermal conductivity of propane

Thermal conductivity of propane was recently [10] determined experimentally in the temperature range from 298 to 373 K and at pressures from 0.9 to 37 MPa. Figure 4 shows the deviation of the present radiation-corrected measurements from NIST [11]. Large deviations between radiation corrected thermal

Table 2 Comparison of thermal properties of nitrogen with Sun [17] and NIST [11]

	NIST [NIST 12, version 5.0]		SUN [Sun, 2002]	
	Average/ %	Maximum/ %	Average/ %	Maximum/ %
λ	+3.1	+3.8	+0.85	+1.6
α	+2	-3.6	+3.3	-10.8
C_p	+3.4	+6.7	+2.2	+4.1

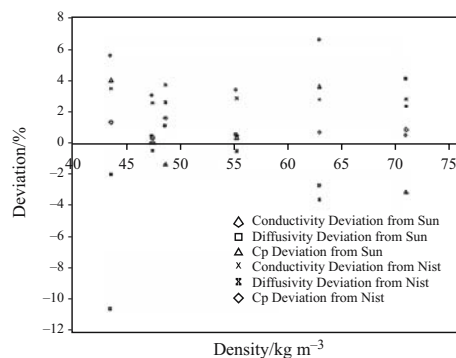


Fig. 3 Comparison of thermal conductivity, thermal diffusivity and specific heat of nitrogen

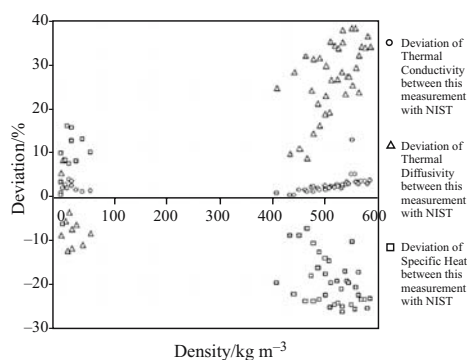


Fig. 4 Comparison of thermal conductivity, thermal diffusivity and specific heat of propane: Radiation-corrected present measurement and NIST data without thermal radiation correction

conductivity and those from NIST [11] is partly attributed to fluid radiation effects not taken into account in these measurements. A close examination of the present experimental data confirms the presence of radiation effects. The procedure to obtain radiation-corrected results is described in the following sections.

Existence of thermal radiation: examination of the experimental data

Presence of fluid radiation effects have been confirmed earlier [9, 10, 14–16] in measurements with *n*-pentane and toluene which are radiation absorbing fluids. This influence is recognized by a curvature in the deviation plot for the linear fit of $\Delta T \sim \ln(t)$ of the experimental data. Such a trend is absent in the deviation plot resulting from a linear fit of $\Delta T \sim \ln(t)$ data in case of radiation free measurements. In these instances, a near perfect linear fit of the corrected temperature-time is obtained as shown in Fig. 5 for argon. Figures 6 and 7 show the deviation plots for *n*-pentane and toluene respectively for both cases, with and without fluid radiation corrections. The curvatures in these deviation plots disappear after the radiation effects are corrected following a correction procedure described in this paper.

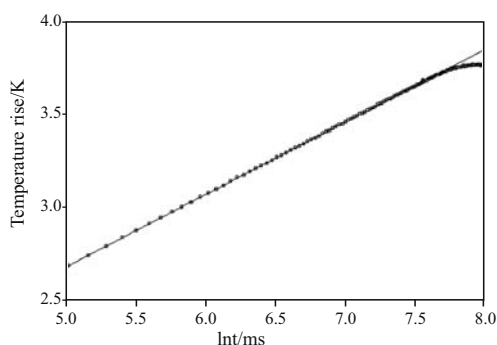


Fig. 5 Temperature rise $\sim \ln(t)$ for a measurement on argon at 323 K and 20.9 MPa

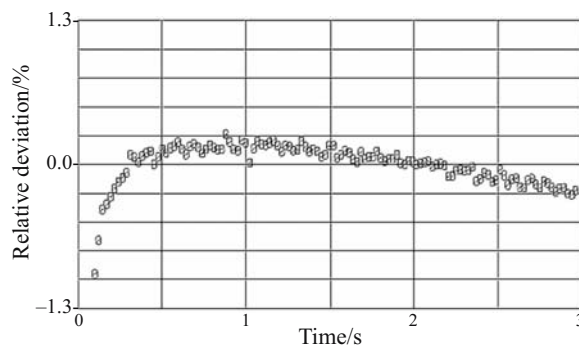


Fig. 8 Deviations plot: linear fit of $\Delta T \sim \ln(t)$ for propane at 373.15 K and 0.9 MPa before radiation correction

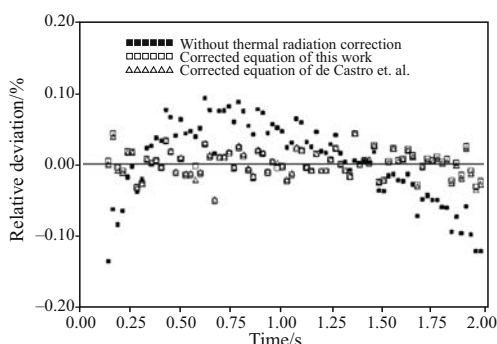


Fig. 6 Deviation plot: linear fit of $\Delta T \sim \ln(t)$ for *n*-pentane at 376 K and 34.17 MPa, before and after radiation correction

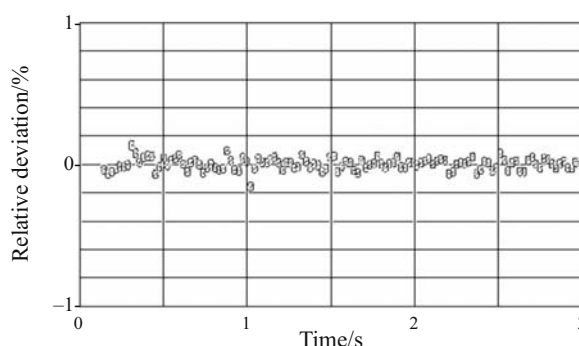


Fig. 9 Deviations plot: linear fit of $\Delta T \sim \ln(t)$ for propane at 373.15 K and 0.9 MPa after radiation correction with $B=0.053$

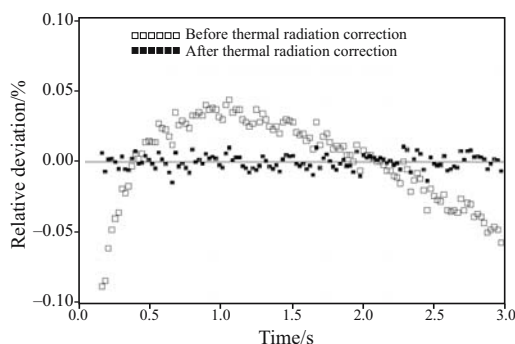


Fig. 7 Deviation plot: linear fit of $\Delta T \sim \ln(t)$ for toluene at 323 K and 20 MPa, before and after radiation correction with $B=0.0088$

A curvature in the deviation plot is also obtained with experimental data obtained in presence of convection. In this case, however, the appearance of the curvature, as shown in Fig. 10 for argon [9, 14, 17], is delayed and $\Delta T \sim \ln(t)$ data shows an excellent fit before the onset of convection. As argon is transparent to thermal radiation, the appearance of curvature in the deviation plot after 1.7 s (Fig. 10) is due to natural convection effects [9]. The curvature in this case is very different from those for propane, *n*-pentane and toluene. The curvatures in case of propane, *n*-pentane and toluene start at the very beginning of the measurement while in case of argon it appears after 1.7 s when Raleigh Number (Ra)

In measurements with propane, a deviation plot (Fig. 7) clearly indicates curvature similar to *n*-pentane and toluene. This indicates the existence of radiation effect in these measurements. Figure 8 shows the deviation plot for propane at 373 K and 881.5 kPa without thermal radiation correction. Figure 9 is the deviation plot for the same data corrected for thermal radiation effect. The application of a suitable thermal radiation and optical parameters B (Eq. (3b)) removes the curvature in case of propane just as it does for *n*-pentane and toluene [15, 16]. It is, therefore, concluded that the measurements on propane are influenced by thermal radiation effects.

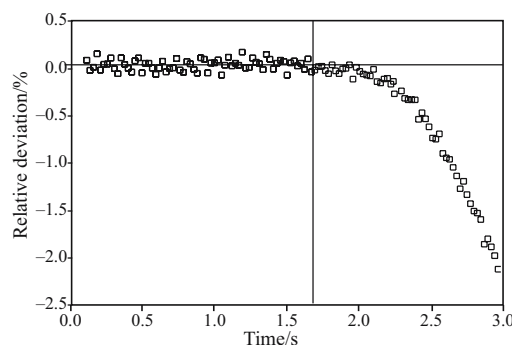


Fig. 10 Deviations plot: linear fit of $\Delta T \sim \ln(t)$ for argon at 323 K and 20.9 MPa

criterion for onset of convection is met as Ra exceeds $1.3 \cdot 10^5$ [9]. These comparisons provide further evidence of the presence of the fluid radiation effects in propane.

Correction for thermal radiation: B-values and curvature in the deviation plot

Radiation free measurements of the thermal properties are obtained using suitable empirical values of B. B is a radiation and optical parameter (Eq. (3b)) outlined earlier [9, 10, 14]. Figures 7 and 8 show the deviation plots obtained from a linear fit of $\Delta T \sim \ln(t)$ data for propane before and after radiation correction. It is seen that use of suitable B values in data processing can effectively remove the curvature in the deviation plot and, therefore, effect of radiation. The experimental data was processed with suitable B values and radiation-corrected thermal conductivity, thermal diffusivity, specific heat and B-values were obtained [10]. The experimental data was also processed with $B=0$ to determine the thermal properties of propane without any fluid radiation correction. In this case, only the thermal conductivity values were determined. It was not possible to obtain a consistent value of the thermal diffusivity and, therefore, the specific heat due to radiation contribution to the experimental data for $\Delta T \sim t$. In the vapor phase at 372 K, 881.5 kPa, the radiation correction is about 4% (Fig. 11, Table 3). The radiation correction in case of liquid propane at 372 K, 15.522 MPa (Fig. 12, Table 4) is much greater (10–28%). Figures 11 and 12 show the deviation between radiation corrected and uncorrected values as a function of q , the power dissipated through the hot wire. Tables 3 and 4 indicate the thermal conductivity of propane before and after correction of radiation effects. The thermal radiation parameter B (Eq. (3b)) is also shown in these Tables.

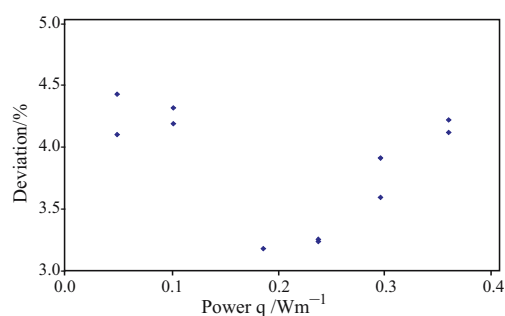


Fig. 11 Radiation correction in thermal conductivity data for propane vapor at 372.33 K, 881.5 kPa

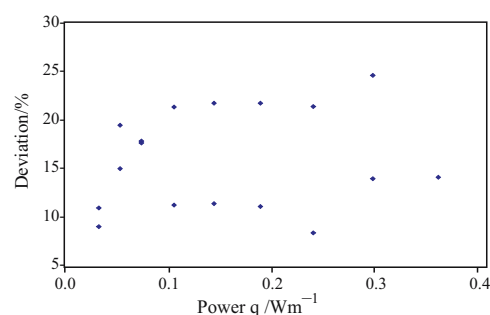


Fig. 12 Radiation correction in thermal conductivity data for liquid propane at 372.05 K, 15.522 MPa

Conclusions

It is shown that fluid radiation effects are present in the measurement of thermal properties of propane using a transient hot-wire instrument. Thermal conductivity values for propane with and without radiation correction are presented to demonstrate the magnitude of the fluid radiation effects in measurements in vapor phase at 372 K, 881.5 kPa and for liquid propane at 372 K 15.522 MPa. The use of suitable values of B, a parameter related to radiation, can effectively

Table 3 Radiation correction for propane vapor at 372 K and 881.5 kPa

FILE ID	T/K	$\rho/\text{kg m}^{-3}$	$q/\text{W m}^{-1}$	B	$\frac{\lambda_{\text{uncorrected}}}{\lambda_{\text{corrected}}}$		Deviation/% $100(\Delta\lambda/\lambda_{\text{corrected}})$
					$\lambda/\text{W m}^{-1} \text{K}^{-1}$		
110021A	373.67	13.479	0.0497	0.09	0.02985	0.02867	4.11
110021B	373.65	13.479	0.0497	0.09	0.02987	0.02860	4.44
11003A	375.06	13.416	0.1028	0.09	0.03000	0.02879	4.20
11003B	375.07	13.415	0.1028	0.09	0.02999	0.02875	4.33
11004A	377.29	13.312	0.1876	0.06	0.03059	0.02965	3.18
110045A	378.65	13.253	0.2397	0.06	0.03097	0.03000	3.24
110045B	378.65	13.251	0.2397	0.06	0.03098	0.03000	3.26
11005A	380.16	13.187	0.2980	0.07	0.03151	0.03042	3.60
11005B	380.16	13.190	0.2981	0.07	0.03150	0.03031	3.92
110055A	381.81	13.118	0.3626	0.06	0.03213	0.03085	4.13
110055B	381.81	13.119	0.3625	0.07	0.03215	0.03084	4.23

Table 4 Radiation correction for liquid propane at 372 K and 15.522 MPa

FILE ID	T/K	$\rho/\text{kg m}^{-3}$	$q/W \text{ m}^{-1}$	B	$\lambda_{\text{uncorrected}}$	$\lambda_{\text{corrected}}$	Deviation/% 100($\Delta\lambda/\lambda_{\text{corrected}}$)
					$\lambda/W \text{ m}^{-1} \text{ K}^{-1}$		
1410015A	372.267	429.464	0.0289	0.15	0.09510	0.08494	11.97
1410015B	372.244	429.500	0.0289	0.20	0.09230	0.08410	9.75
1410021A	372.346	429.271	0.0497	0.30	0.09960	0.08536	16.68
1410021B	372.393	429.341	0.0497	0.30	0.10213	0.08385	21.80
1410025A	372.525	429.075	0.0704	0.30	0.10082	0.08407	19.93
1410025B	372.520	429.081	0.0704	0.30	0.10100	0.08438	19.69
141003A	372.736	428.762	0.1027	0.20	0.09426	0.08390	12.34
141003B	372.717	428.782	0.1027	0.36	0.10476	0.08449	24.00
1410035A	372.990	428.369	0.1418	0.37	0.10403	0.08360	24.44
1410035B	372.990	428.383	0.1418	0.20	0.09472	0.08418	12.52
141004A	373.300	427.908	0.1873	0.30	0.09468	0.08442	12.15
141004B	373.270	427.893	0.1872	0.36	0.10429	0.08380	24.45
1410045A	373.610	427.417	0.2392	0.36	0.10478	0.08446	24.05
1410045B	373.650	427.402	0.2392	0.15	0.09316	0.08548	8.98
141005A	374.040	426.762	0.2974	0.24	0.09869	0.08547	15.46
141005B	374.000	426.807	0.2972	0.40	0.10792	0.08448	27.75
1410055B	374.460	426.121	0.3615	0.24	0.09953	0.08609	15.61

correct thermal radiation influence. Comparison of the radiation corrected data with NIST indicates significant difference some of which is attributed to radiation effects. Further investigation of the reasons for large deviations is proposed.

Acknowledgements

The work was performed under a program of studies funded by the Natural Sciences and Engineering Research Council of Canada, under Grant number A8859 and A5477.

References

- 1 S. C. Mojumdar and L. Raki, *J. Therm. Anal. Cal.*, 82 (2005) 89.
- 2 S. C. Mojumdar and L. Raki, *J. Therm. Anal. Cal.*, 85 (2006) 99.
- 3 X. Qiu, N. Mathis and K. Schimdt, *Thermochim. Acta*, in press.
- 4 B. Chowdhury and S. C. Mojumdar, *J. Therm. Anal. Cal.*, 81 (2005) 179.
- 5 S. C. Mojumdar, *J. Therm. Anal. Cal.*, 64 (2001) 1133.
- 6 B. Chowdhury, *J. Therm. Anal. Cal.*, 78 (2004) 215.
- 7 S. C. Mojumdar, L. Raki, N. Mathis, K. Schmidt and S. Lang, *J. Therm. Anal. Cal.*, 85 (2006) 119.
- 8 J. J. Healy, J. J. De Groot and J. Kestin, *Physica*, 82C (1976) 392.
- 9 L. Sun, Simultaneous Measurement of Thermal Conductivity and Thermal Diffusivity, PhD Thesis, University of New Brunswick, Fredericton, NB, Canada (2001).
- 10 Y. Shi, Radiation Effects in Transient Hot-Wire Technique: Simultaneous Measurement of Thermal Conductivity and Diffusivity of Propane, MScE Thesis, University of New Brunswick, Saint John, NB, Canada (2006).
- 11 E. W. Lemmon, A. P. Peskin, M. O. Melinden and D. G. Friend, NIST Standard Reference Data Base 12, Version 5. The U.S. Secretary of Commerce on Behalf of the United States of America.
- 12 J. Menashe and W. A. Wakeham, *Int. J. Heat Mass Tr.*, 25 (1982) 661.
- 13 L. Sun and J. E. S. Venart, *Int. J. Thermophys.*, 26 (2005) 325.
- 14 Y. Shi, L. Sun, J. E. S. Venart and R. C. Prasad, *J. Therm. Anal. Cal.*, 86 (2006) 585.
- 15 L. Sun, J. E. S. Venart and R. C. Prasad, *Int. J. Thermophys.*, 23 (2002) 391.
- 16 L. Sun, J. E. S. Venart and R. C. Prasad, *Int. J. Thermophys.*, 23 (2002) 1487.
- 17 L. Sun, J. E. S. Venart and R. C. Prasad, *Int. J. Thermophys.*, 23 (2002) 357.

DOI: 10.1007/s10973-007-8524-7